# The effect of excitation and preparation pulses on nonslice selective 2D UTE bicomponent analysis of bound and free water in cortical bone at 3T

Shihong Li
*Department of Radiology, University of California, San Diego, California 92103-8226; Department of Radiology, Hua Dong Hospital, Fudan University, Shanghai 200040, China; Yancheng Medical College, Jiangsu, China; and The First People's Hospital of Yancheng City, Jiangsu 224005, China*

Eric Y. Chang
*VA San Diego Healthcare System, San Diego, California 92161 and Department of Radiology, University of California, San Diego, California 92103-8226*

Won C. Bae
*Department of Radiology, University of California, San Diego, California 92103-8226*

Christine B. Chung
*VA San Diego Healthcare System, San Diego, California 92161 and Department of Radiology, University of California, San Diego, California 92103-8226*

Yanqing Hua
*Department of Radiology, Hua Dong Hospital, Fudan University, Shanghai 200040, China*

Yi Zhou
*The First People's Hospital of Yancheng City, Jiangsu 224005, China*

Jiang Du[a)]
*Department of Radiology, University of California, San Diego, California 92103-8226*

(Received 21 July 2013; revised 15 November 2013; accepted for publication 8 January 2014; published 27 January 2014)

**Purpose:** The purpose of this study was to investigate the effect of excitation, fat saturation, long T2 saturation, and adiabatic inversion pulses on ultrashort echo time (UTE) imaging with bicomponent analysis of bound and free water in cortical bone for potential applications in osteoporosis.
**Methods:** Six bovine cortical bones and six human tibial midshaft samples were harvested for this study. Each bone sample was imaged with eight sequences using 2D UTE imaging at 3T with half and hard excitation pulses, without and with fat saturation, long T2 saturation, and adiabatic inversion recovery (IR) preparation pulses. Single- and bicomponent signal models were utilized to calculate the T2*s and/or relative fractions of short and long T2*s.
**Results:** For all bone samples UTE T2* signal decay showed bicomponent behavior. A higher short T2* fraction was observed on UTE images with hard pulse excitation compared with half pulse excitation (75.6% vs 68.8% in bovine bone, 79.9% vs 73.2% in human bone). Fat saturation pulses slightly reduced the short T2* fraction relative to regular UTE sequences (5.0% and 2.0% reduction, respectively, with half and hard excitation pulses for bovine bone, 6.3% and 8.2% reduction, respectively, with half and hard excitation pulses for human bone). Long T2 saturation pulses significantly reduced the long T2* fraction relative to regular UTE sequence (18.9% and 17.2% reduction, respectively, with half and hard excitation pulses for bovine bone, 26.4% and 27.7% reduction, respectively, with half and hard excitation pulses for human bone). With IR-UTE preparation the long T2* components were significantly reduced relative to regular UTE sequence (75.3% and 66.4% reduction, respectively, with half and hard excitation pulses for bovine bone, 87.7% and 90.3% reduction, respectively, with half and hard excitation pulses for human bone).
**Conclusions:** Bound and free water T2*s and relative fractions can be assessed using UTE bicomponent analysis. Long T2* components are affected more by long T2 saturation and IR pulses, and short T2* components are affected more by fat saturation pulses. © *2014 American Association of Physicists in Medicine*. [http://dx.doi.org/10.1118/1.4862838]

Key words: ultrashort TE, bound water, free water, fat saturation, long T2 saturation, adiabatic inversion recovery, cortical bone, MRI

## 1. INTRODUCTION

Osteoporosis (OP) is a worldwide public health problem.[1] It is routinely assessed with dual-energy x-ray absorptiometry (DEXA), which measures bone mineral density (BMD). However, BMD has been shown to be a poor predictor of osteoporotic fracture.[2,3] It is known that bone strength is dependent on the quality and integration of all the major

components, not only the mineralized portion. This includes the organic matrix and bone water, which are not assessed by DEXA, but occupy approximately 60% of bone by volume.[4]

Bone water makes significant contribution to the biomechanical properties of cortical bone and has been studied extensively.[5–9] Quantifying water in cortical bone is an important factor in assessing bone quality.[10] Magnetic resonance imaging (MRI) has been widely used to diagnose musculoskeletal diseases including osteoporosis,[11,12] but conventional clinical MRI sequences cannot detect the water signal from cortical bone.[6,13,14] Water in cortical bone mainly exits in three states: free water which moves freely in microscopic pores and the Haversian and lacunocanalicular system, water loosely bound to the organic matrix, and water tightly bound to mineral. Bound water concentration provides an indirect measure of organic matrix density.[15] Free water concentration can potentially provide a surrogate measure of cortical porosity.[16,17] Bound and free water make different contributions to the mechanical properties of bone,[18] highlighting the importance of separating the two in studies of bone quality. Techniques capable of bound and free water quantification demonstrate considerable potential for improving clinical diagnosis and monitoring treatment.

Recently, multicomponent analysis of Carr–Purcell–Meiboon–Gill (CPMG) spin echo and free induction decay (FID) data from high performance NMR spectrometers have been used to provide T2 or T2* spectra which reflect tightly bound water with a T2* of less than 10 $\mu$s, loosely bound water with a T2* of 0.3–0.5 ms and free water with a T2* of 2–5 ms.[15–19] More recently the ultrashort echo time (UTE) sequence with a minimal nominal TE of 8 $\mu$s together with bicomponent analysis of UTE T2* signal decay has been employed to quantify both loosely bound water and free water using a whole body clinical scanner.[20–22] For this paper, we will refer to loosely bound water as bound water from now on. Preliminary studies at 1.5 and 3 T suggest that UTE bicomponent analysis provides consistent measures of bound and free water fractions, thereby allowing field-independent comparisons.[21]

However, signal from distinct bone water compartments is affected differently by multiple factors, including radiofrequency (RF) excitation and preparation pulses.[22] This is particularly important for *in vivo* bone imaging, which usually requires efficient suppression of signal from surrounding muscle and fat. These tissues have much longer T2s and higher proton densities than cortical bone. Visualization of cortical bone can be significantly compromised without suppression of the signal from these tissues due to lack of contrast and suboptimal dynamic range. The long T2 suppression pulses used to achieve this are likely to affect the quantification of bound and free water in cortical bone. To the best of our knowledge, the effect of RF excitation and preparation pulses on the quantification of bound and free water in cortical bone is not known.

To address this issue, we investigated the effect of RF excitation pulse shape (hard rectangular pulse versus the commonly used half sinc pulse) as well as preparation pulses including fat saturation pulse, long T2 saturation, and adiabatic inversion recovery (IR) on UTE bicomponent analysis of bound and free water in bovine and human cortical bone samples.

## 2. MATERIALS AND METHODS

### 2.A. Sample preparation

Six mature bovine femoral midshaft bone samples from freshly slaughtered animals were obtained from a local slaughterhouse and cleaned of external muscle and soft tissue. Six cadaveric human tibial midshaft bone samples from six donors (without detailed demographic information or record of the cause of death) were harvested from cadaveric leg specimens obtained from the University of California, San Diego (UCSD) morgue. These were also cleared of external muscle and soft tissue. Bone marrow in all bone samples was removed with a scalpel. The bovine cortical bone was cut into $10 \times 10 \times 10$ mm$^3$ (length $\times$ width $\times$ height) samples under constant saline irrigation using a low-speed precision circular diamond-edge saw (Isomet 1000, Buehler, Lake Bluff, IL). Cross-sectional human cortical bone segments were cut transversely to an approximate thickness of 20–30 mm. Individual samples were placed in phosphate buffered saline (PBS) solution for 24 h and stored at 4 °C prior to MR imaging. The samples were equilibrated to room temperature (21 °C) before imaging.

### 2.B. Pulse sequences

The bovine and human cortical bone samples were subject to nonslice selective 2D UTE imaging using a 3T Signa Twin-Speed scanner (GE Healthcare Technologies, Milwaukee, WI). The scanner has a maximum gradient strength of 40 mT/m and a maximum slew rate of 150 mT/m ms. Figure 1 shows the basic 2D UTE pulses sequences that were used. These had a short rectangular pulse excitation [duration = 32 $\mu$s, Fig. 1(a)] or a short half sinc pulse excitation [duration = 472 $\mu$s, bandwidth = 2.7 kHz, Fig. 1(b)]. The slice selection gradient was set to zero for nonslice selective excitation. This reduced scan time and minimized the eddy currents associated with conventional 2D UTE imaging. The basic nonselective 2D UTE sequence was combined with three different preparation pulses, namely, a conventional chemical shift based fat saturation pulse (pulse duration = 3.2 ms, pulse bandwidth = 280 Hz, pulse frequency offset = −440 Hz, nominal flip angle = 94°), a long T2 saturation pulse (Gaussian pulse, pulse duration = 8 ms, pulse bandwidth = 2 kHz), and an adiabatic inversion pulse (Silver-Hoult pulse, pulse duration = 8.64 ms, pulse bandwidth = 1.4 kHz, pulse peak power = 12 $\mu$T). Preparation pulses were varied in order to investigate their effects on bound and free water quantification. Nonslice selective 2D excitation was used to eliminate errors due to eddy currents associated with conventional slice selective half-pulse excitation. This also speeds up data acquisition since only one excitation is needed for nonselective excitation compared with two excitations which are required for slice-selective excitation.

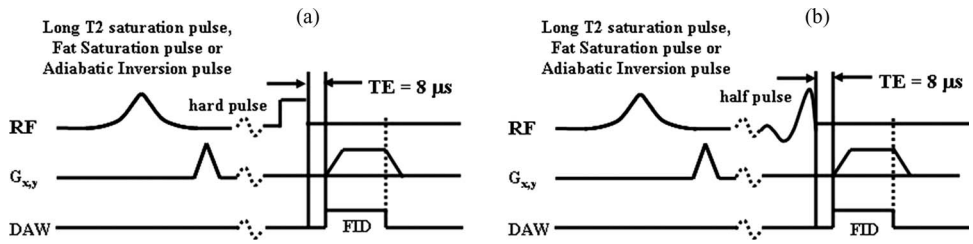


FIG. 1. 2D nonselective UTE imaging with rectangular (a) or half (b) pulse excitation. The basic UTE sequences can be preceded by long T2 saturation, fat saturation, or adiabatic inversion pulses.

### 2.C. MR data acquisition

A home-built birdcage coil (~2.5 cm in diameter) was used for signal excitation and reception. Each bone sample was placed in a 30 ml syringe filled with Fomblin (Solvay Solexis, West Deptford, NJ) during MR imaging in order to maintain hydration and minimize susceptibility effects at air-bone junctions. The basic 2D UTE imaging protocol employed the following parameters: TR = 300 ms, flip angle = 20°, field of view (FOV) = 8 cm, reconstruction matrix = 256 × 256, number of projections = 255 (actual sampling points = 136), sequentially ordered, gradient spoiling, bandwidth = 125 kHz, sampling window = 1088 $\mu$s, 20 TEs (0.01, 0.1, 0.2, 0.3, 0.4, 0.5, 0.6. 0.8, 1.0, 1.2, 1.4, 1.6, 2, 2.5, 3, 4, 5, 6, 7, and 8 ms). The acquisition time was approximately 1.3 min per image. Relatively long TRs and low flip angles were used to minimize T1 effects (~98% signal recovery could be achieved with a TR of 300 ms, a T1 of 200 ms, and a flip angle of 20°) as well as specific absorption ratio (SAR). The bone specimens were expected to remain in room temperature during the whole scanning process. Each of four preparations none, fat suppression (FS), long T2 saturation (SAT), or inversion recovery (IR) were combined with one of the two excitations hard (hard) or half sinc (half) for eight total sequence variations. Each bone sample was placed near the center of the birdcage coil to minimize adverse effects due to coil radiofrequency field inhomogeneity (variation less than 3%). The 2D nonselective axial imaging plane was centered in the middle of each sample so that the UTE signal intensity represented the integrated signal across the whole bone axial thickness. One human bone specimen was imaged five times on five different days. The reproducibility was estimated with coefficients of variation calculated as the ratio of the standard deviation to the average UTE bicomponent analysis values.

### 2.D. MR image analysis

A semiautomated Matlab (The Mathworks Inc., Natick, MA) code was written for the UTE single- and bicomponent analysis of the magnitude signals. The program allowed placement of regions of interest (ROIs) on the first image of the series, which were then copied to the corresponding position on each of the subsequent images. The mean intensity within each of the ROIs was used for subsequent curve fitting. In single-component analysis the UTE signals $S_N(t)$ were fitted with the following equation:

$$S_N(t) = A \times e^{-t/T_2^*} + \text{noise}. \quad (1)$$

In bicomponent analysis the UTE signals $S_N(t)$ were fitted with the following commonly used model [Eq. (2)]:

$$S_N(t) = A_S \times e^{-t/T_{2S}^*} + A_L \times e^{-t/T_{2L}^*} + \text{noise}, \quad (2)$$

where $T_{2S}^*$ is the short water T2*, $T_{2L}^*$ is the long water T2*, and $A_S$ and $A_L$ are the signal amplitudes of the short and long $T_2^*$ components. Apparent bound water fraction was defined as $A_S/(A_S + A_L)$.

Background noise was automatically estimated using a maximum likelihood estimation (MLE) distribution fitting of a partial histogram. Non-negative least-square curve fitting was employed for both single- and bicomponent model. More details about the UTE bicomponent analysis technique can be found in Ref. 20. Five different ROIs were fitted to determine the average UTE bicomponent analysis values.

## 3. RESULTS

Figure 2 shows selected UTE images of a human bone segment with hard excitation pulse and TEs of 10 $\mu$s (a), 0.2 ms (b), 0.4 ms (c), 0.6 ms (d), 0.8 ms (e), 1.2 ms (f), 1.6 ms (g), 2.0 ms (h), 3.0 ms (i), 4.0 ms (j), 5.0 ms (k), and 6.0 ms (l), single- (m), and bicomponent (n) fitting and the corresponding fitting residuals (o) and (p). Single-component fitting of the UTE T2* decay curve from a ROI drawn in cortical bone shows a short T2* value of 0.67 ms, however, there is a large residual signal, which is over 10% at a TE of 3 ms, suggesting the existence of another water component. The residual signal is reduced to less than 0.5% through bicomponent fitting, which shows a shorter T2* of 0.39 ms and a longer T2* of 2.66 ms with respective fractions of 76.9% and 23.1% by volume. This demonstrates that the bicomponent analysis model is well suited for depicting the UTE T2* decay behavior of cortical bone. There are two observed components with the short T2* component corresponding to bound water and the long T2* component corresponding to free water. The average coefficients of variation for bound water T2* and fraction on six repeated acquisitions were 2.6% and 3.9%, respectively. These results show that the UTE bicomponent analysis technique provides reliable quantification for bound and free water T2*s as well as their fractions.

Figure 3 shows the single- and bicomponent analysis of UTE images of a bovine bone sample acquired with eight different acquisition schemes. Comparison of the T2*s of bound water demonstrates no change or negligible change between

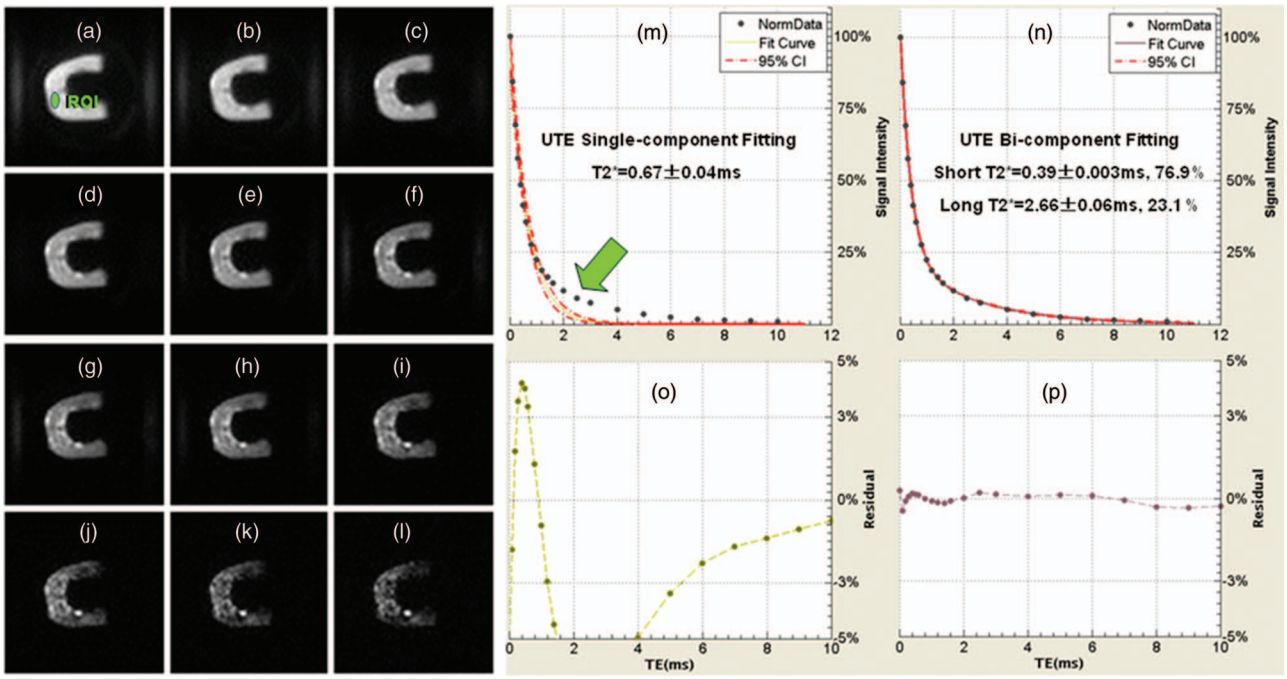


FIG. 2. Selected UTE imaging of a human cortical bone sample with TEs of 10 $\mu$s (a), 0.2 ms (b), 0.4 ms (c), 0.6 ms (d), 0.8 ms (e), 1.2 ms (f), 1.6 ms (g), 2.0 ms (h), 3.0 ms (i), 4.0 ms (j), 5.0 ms (k), and 6.0 ms (l), single- (m) and bicomponent (n) fitting with the corresponding fitting residuals (o) and (p). Single-component fitting shows significant residual signal (>10%) (o). The residual signal is reduced to less than 0.5% by bicomponent fitting (p). This gives a shorter T2* of 0.39 ms and a longer T2* of 2.66 ms with respective fractions of 76.9% and 23.1% by volume (N).

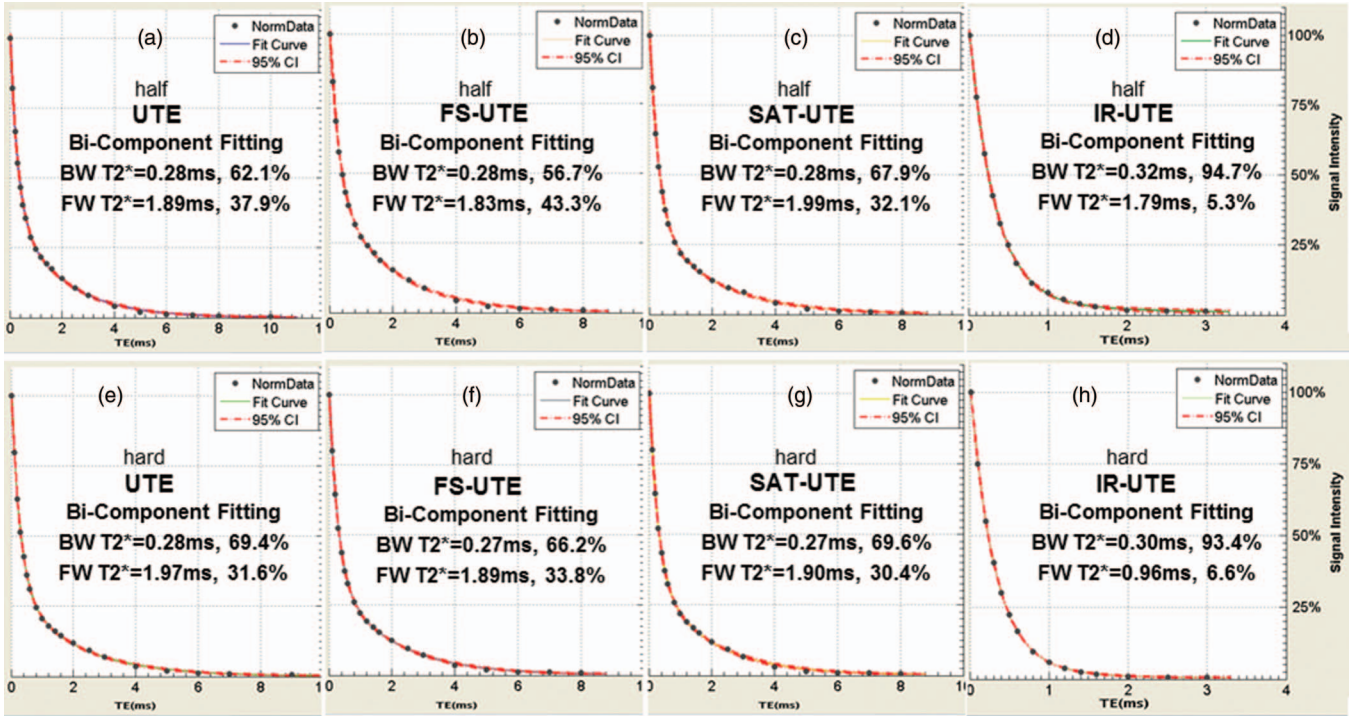


FIG. 3. Bicomponent analysis of UTE images of a bovine bone acquired with a half-excitation pulse (first row) and hard rectangular excitation pulse (second row) without preparation pulse (a) and (e), with a fat saturation pulse (FS-UTE) (b) and (f), a long T2 saturation pulse (SAT-UTE) (c) and (g), and an adiabatic inversion recovery pulse (IR-UTE) (d) and (h). BW and FW represent bound water and free water. CI means the confidence interval. The bicomponent analysis shows that BW T2*s (short T2*s) are similar between half and hard pulses, FW T2*s (long T2*s) ranged from 0.96 to 1.99 ms. The bound water fraction increases from 56.7% with the fat saturation pulse (b), to 62.1% with no preparation pulse (a), to 67.9% with the long T2 saturation pulse (c), and to 94.7% with inversion recovery pulse (d). In the hard pulse excitation group (second row), the bound water fraction followed a similar trend and increased from 66.2% with the fat saturation pulse (f), to 69.4% with no preparation pulse (e), to 69.6% with the long T2 saturation pulse (g), and to 93.4% with inversion recovery pulse (h).

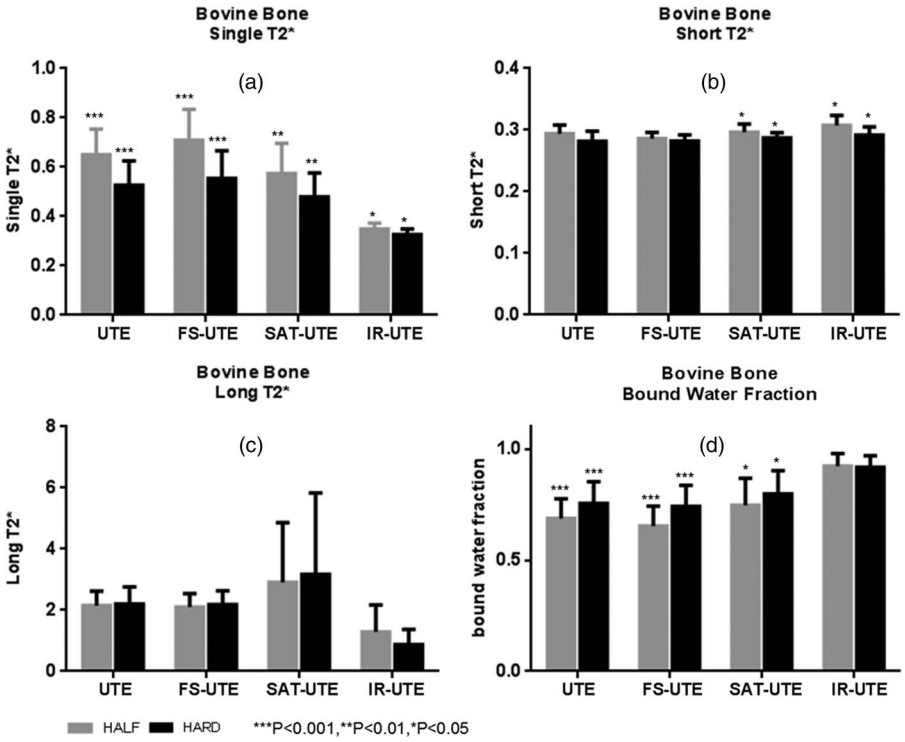


FIG. 4. Summary of all bovine cortical bone samples with mean single component T2*s (a), mean short T2*s (b), mean long T2*s (c), and mean bound water fractions (d). Gray and black rectangular, respectively, present half and hard excitation pulses. The stars on the error bars represented the *t*-test results of the same group. Single-component analysis demonstrated mean T2*s ranging from 0.33 to 0.71 ms (a) with the different pulse sequences. Bicomponent analysis provided mean short T2*s ranging from 0.28 to 0.31 ms (b), mean long T2*s ranging from 0.87 to 3.17 ms (c), and bound water fractions ranging from 65.3% to 92.3% (d) across the eight different acquisition modes.

half and hard UTE (a) and (e), FS-UTE (b) and (f), and SAT-UTE (c) and (G) pulses. The short T2*s were 0.28–0.32 ms for the half pulse excitations, and between 0.27 and 0.30 ms for the hard pulse excitations. Similarly, there was a very small change between the T2*s of free water. The apparent fractions indicated large variation with different pulses. All of the apparent bound water fractions from the hard pulse excitations were significantly higher ($p < 0.05$) than those from the half pulse excitations with the exception of a nonstatistically significant decrease with IR-UTE. This shows that the bound water components with shorter T2*s can be more efficiently excited with a short hard pulse compared with a longer half pulse, regardless of preparation pulse. In the half pulse excitation group (first row), the apparent bound water fraction increases from 56.7% in FS-UTE (b), to 62.1% in UTE (a), to 67.9% in SAT-UTE (c), to 94.7% in IR-UTE (d) sequences. In the hard pulse excitation group (second row), the apparent bound water fraction followed a similar trend and increased from 66.2% in FS-UTE (f), to 69.4% in UTE (e), to 69.6% in SAT-UTE (g), and to 93.4% in IR-UTE (h) sequences.

Figure 4 shows a summary of the mean single component T2*s, short T2*s, long T2*s, and apparent bound water fractions for all bovine cortical bone samples. Single-component analysis demonstrated mean T2*s ranging from 0.33 to 0.71 ms with the different pulse sequences. Mean short T2*s ranged from 0.28 to 0.31 ms, mean long T2*s ranged from 0.87 to 3.17 ms, and bound water fractions ranged from 65.3% to 92.3% across the eight different acquisition modes. A higher apparent bound water fraction was observed with UTE images using hard pulse excitations compared with half pulse excitation (75.6% vs 68.8%, $p < 0.001$). Fat saturation pulses showed an apparent bound fraction of 65.3% with half pulses and 74.1% with hard pulses ($p < 0.001$). Relative to regular UTE sequences these fractions were lower by 5% and 2%, respectively. Long T2 saturation pulse suppressed free water by 18.9% for half pulse and 17.2% for hard pulse relative to the regular UTE sequence. Correspondingly, the apparent bound water fractions were increased to 74.7% for half pulse excitation and 79.8% for hard pulse excitation ($p < 0.05$). In IR-UTE the long T2* components were decreased by 75.3% with half pulse excitation and 66.4% with hard pulse excitation. Paired samples two-tailed *t*-test found significant differences between the single component T2*s of half UTE and hard UTE ($p < 0.001$), half FS-UTE and hard FS-UTE ($p < 0.001$), half SAT-UTE and hard SAT-UTE ($p < 0.01$), and half IR-UTE and hard IR-UTE ($p < 0.05$) (a). The short T2*s between half SAT-UTE and hard SAT-UTE as well as half IR-UTE and hard IR-UTE also show significant differences (both $p < 0.05$) (b). No significant differences were found between the remaining paired samples ($p > 0.05$).

Figure 5 shows a summary of the mean single component T2*s, short T2*s, long T2*s, and apparent bound water fractions for all human cortical bone samples. Single-component analysis demonstrated T2*s ranging from 0.38s to 0.79 ms with the different pulse sequences. Bicomponent analysis showed the mean short T2*s ranged from 0.31 to

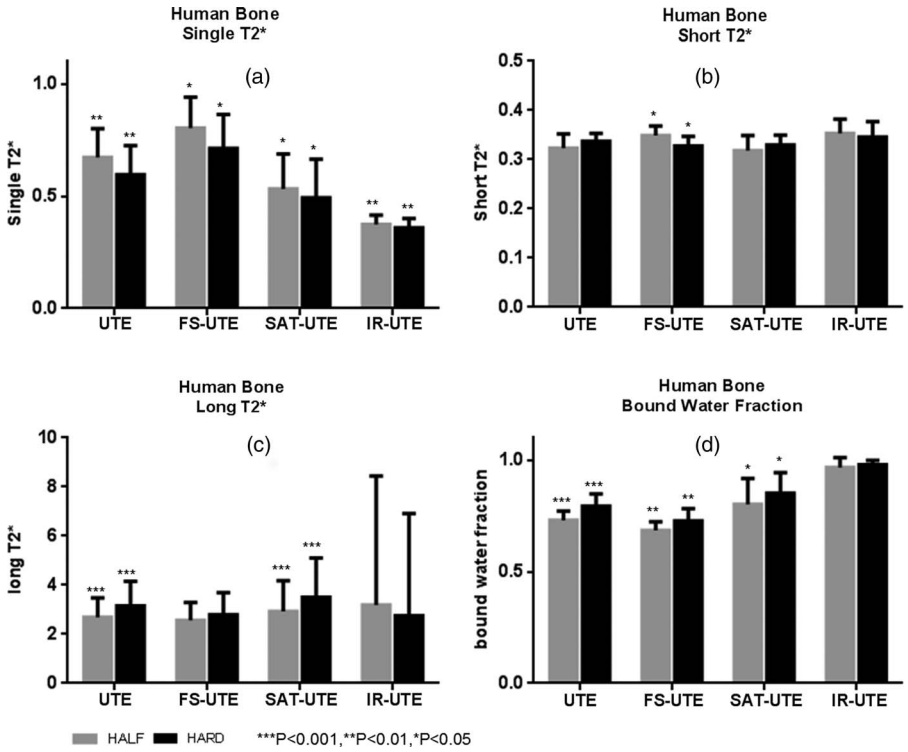


FIG. 5. Summary of all human cortical bone samples with mean single component T2*s (a), mean short T2*s (b), mean long T2*s (c), and mean bound water fractions (d). Gray and black rectangular, respectively, represent half and hard excitation pulses. The stars on the error bars represent the *t*-test results of the same group. Single-component analysis demonstrated T2*s ranging from 0.38 to 0.79 ms (a) with the different pulse sequences. Bicomponent analysis provided mean short T2*s ranging from 0.31 to 0.36 ms (b), mean long T2*s ranging from 1.56 to 2.14 ms (c), and bound water fractions ranging from 64.8% to 95.1% (d) across the eight different acquisition modes.

0.36 ms, mean long T2*s ranged from 1.56 to 2.14 ms, and bound water fractions ranged from 64.8% to 95.1% across the eight different acquisition modes. The apparent bound water fraction observed from UTE images with hard pulse excitation is higher than that with half pulse excitation (79.4% vs 73.1%, $p < 0.001$). The fat saturation pulse induces a decrease in the apparent bound water fraction relative to the nonfat saturated half and hard UTE, respectively, by 6.3% and 8.2% ($p < 0.01$). The long T2 saturation pulse suppresses 26.4%–27.7% more of the free water fraction compared with the regular UTE pulse, causing a rise in the apparent bound water fraction to 80.2%–85.1% ($p < 0.05$). In IR-UTE, the long T2* components demonstrated a nonsignificant increase from 87.7% with half IR-UTE to 90.3% with hard IR-UTE ($p > 0.05$). Paired samples two-tailed *t*-test found significant differences between the single component T2*s of half UTE and hard UTE ($p < 0.01$), half FS-UTE and hard FS-UTE ($p < 0.05$), half SAT-UTE and hard SAT-UTE ($p < 0.05$), and half IR-UTE and hard IR-UTE ($p < 0.01$). The short T2*s between half FS-UTE and hard FS-UTE also showed a significant difference ($p < 0.05$). Significant differences were also found between the long T2*s of half UTE and hard UTE ($p < 0.001$) as well as between half SAT-UTE and hard SAT-UTE ($p < 0.001$) (c). No significant differences were found between the remaining paired samples ($p > 0.05$).

Figure 6 shows a box plot of the apparent bound water fractions from bovine (a) and human (b) cortical bones samples. In the bovine group, two-tailed *t*-tests found significant differences between half UTE and half FS-UTE ($p < 0.01$), half FS-UTE and half SAT-UTE ($p < 0.05$), hard UTE and hard FS-UTE ($p < 0.05$), and hard FS-UTE and hard SAT-UTE ($p < 0.05$). However, there were no significant differences between half UTE and half SAT-UTE ($p > 0.05$), and hard UTE and hard SAT-UTE ($p > 0.05$). In human bone group, two-tailed *t*-tests showed significant differences between half UTE and half FS-UTE ($p < 0.001$), half FS-UTE and half SAT-UTE ($p < 0.05$), hard UTE and hard FS-UTE ($p < 0.01$), and hard FS-UTE and hard SAT-UTE ($p < 0.01$). No significant differences were found between half UTE and half SAT-UTE ($p > 0.05$), and hard UTE and hard SAT-UTE ($p > 0.05$).

## 4. DISCUSSION

UTE sequences allow signal detection from short T2 structures such as menisci, tendons, ligaments, and cortical bone by acquiring the data as soon as possible following the radiofrequency excitation pulse.[14] However, the signal acquired is a combination of both short and long T2 components. In order to achieve superior contrast and highlight the short T2 components, signal from fat and other surrounding long T2 tissues may need to be suppressed using a frequency selective pulse centered on the main fat peak (fat saturation), application of a frequency selective pulse centered on the main water peak (long T2 saturation pulse), or through an adiabatic inversion recovery pulse.[23–25] Also of great interest is the quantitative assessment of short T2 tissues, including their short

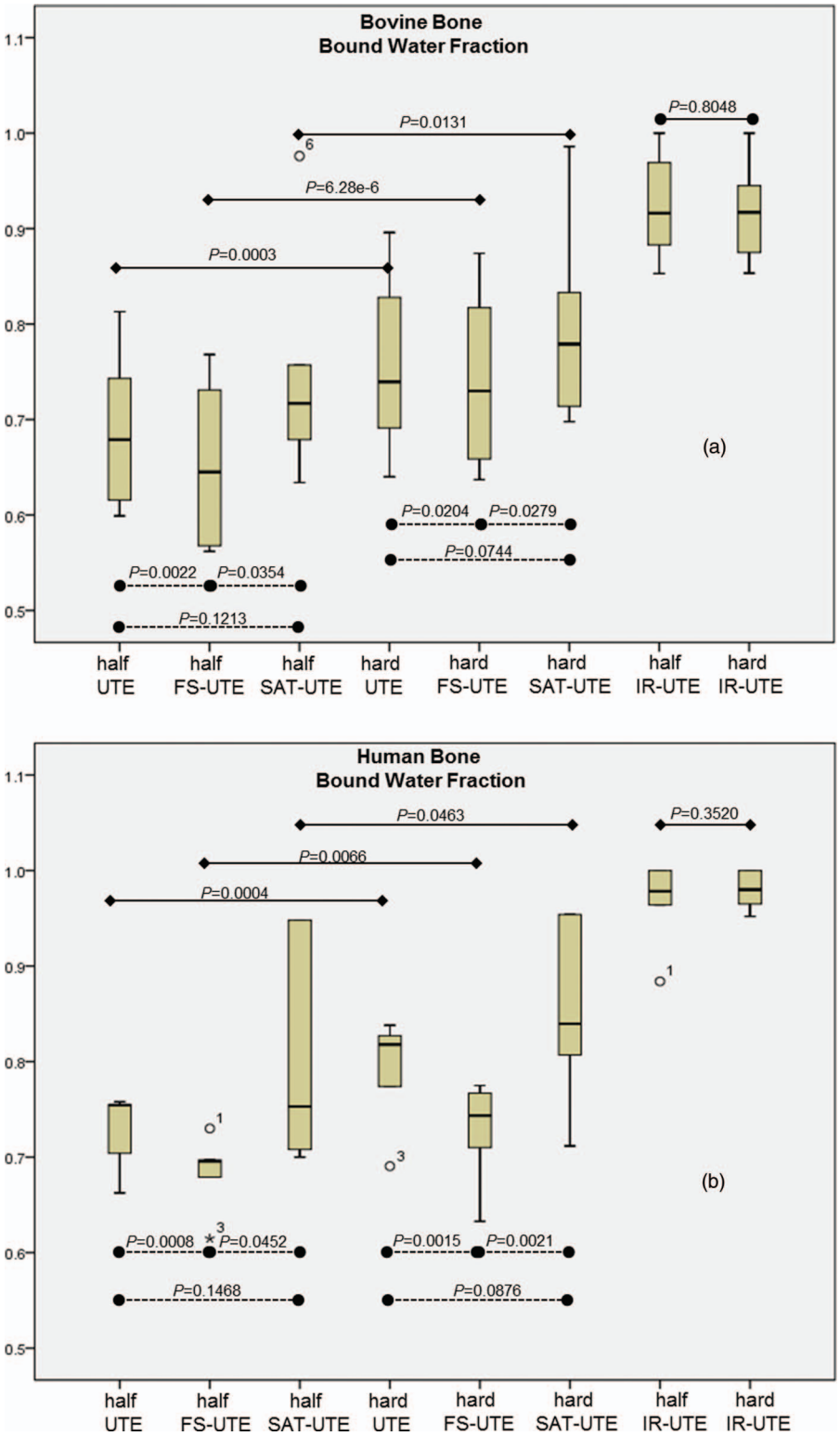


FIG. 6. Box plot showing the bound water fraction in bovine (a) and human (b) cortical bone samples. Solid lines represent the comparison results between half and hard pulses, while the dotted lines represent the comparison between different preparation pulse. In two groups of bones, two-tailed *t*-test found the bound water fraction had significant differences between half UTE and half FS-UTE, half FS-UTE and half SAT-UTE, hard UTE and hard FS-UTE, and hard FS-UTE and hard SAT-UTE (all with $p$ values $< 0.05$).

and long T2*s and relative fractions. Multicomponent fitting models have been used for this purpose, but may not be clinically viable due to the exquisite sensitivity of the technique to signal-to-noise ratio (SNR), number of fitting components, distribution of TEs, and differences between T2 values of the individual components.[26–28] A number of these limitations can be addressed using a bicomponent fitting model.[29] The resultant decreased sensitivity of the results to SNR allows *in vivo* imaging. Prior to clinical translation, however, an understanding of the variables that can affect the results of

quantitative MRI is necessary. Recently we have studied the effect of field strength and found that although the short and long T2* values of cortical bone decrease with increasing field strength (1.5–3 T), the bound water fractions remained unchanged.[21] For the current study, we varied the excitation (half-sinc versus hard rectangular) and preparation pulses (no preparation, fat saturation, and long T2 saturation) and observed the effects on short T2*, long T2*, and bound water fraction.

As with previous studies,[30] our results show that single component fitting cannot adequately explain the UTE T2* signal decay behavior (Fig. 2). However, the bicomponent fitting model is well suited for analysis of the acquired signal, which demonstrated two distinct components: one with a short T2* of 0.39 ms and the other with a long T2* of 2.66 ms for this sample of human cortical bone. The shorter T2* component accounted for 76.9% of the total UTE MR signal decay, and the longer T2* component accounted for the other 23.1% of the signal decay. The values obtained in this study are comparable to those published in multiple previous studies.[16–18,30,31] However, as Fig. 3 demonstrates, the precise quantitative values are dependent on the type of excitation and preparation pulses used. In general, bound water fractions are greater with hard excitation pulses compared to these with half excitation pulses. This is likely due to the greater degree of bound water excitation produced by the hard excitation pulses, which have higher power and shorter duration than half sinc pulses and thus are more efficient in exciting tissues or tissue components with extremely short T2*s.[22]

UTE with different preparation pulses also demonstrates consistent effects. For instance, with fat saturation preparation pulses, a radiofrequency pulse is delivered to cover the main fat resonance frequency with subsequent gradient spoiling to suppress the fat signal. Unfortunately there is also inadvertent suppression of some short T2* signal from bound water as well, due to overlapping frequencies. Specifically, although long T2 tissues such as muscle, articular cartilage, liver, white matter, and gray matter demonstrate relatively narrow spectral linewidths (typically $<$10 Hz), short T2 species such as tendon, meniscus, calcified cartilage, cortical bone, and myelin have much broader linewidths (ranging from hundreds to thousands of hertz).[32,33] Both bound and free water have relative short T2* and are both affected by the fat saturation pulse. However, signal from bound water with approximately 10 times shorter T2* is suppressed more by the fat saturation pulse than that of free water. This explains the trend toward lower apparent bound water fraction (5.0% and 2.0% reduction, respectively, with half and hard excitation pulses for bovine bone, 6.3% and 8.2% reduction, respectively, with half and hard excitation pulses for human bone) seen with fat saturation pulses compared to imaging without these pulses.

With long T2 saturation preparation pulses, a radiofrequency pulse is delivered to cover the main, narrow water frequency with subsequent gradient spoiling to suppress the long T2 water signal, leaving the short T2 water signal being selectively detected by the UTE sequences. As with fat suppression pulses, bound water components will show some degree of suppression due to overlapping frequencies. However, the free water component will be more efficiently suppressed by the long T2 saturation preparation pulses compared to the bound water component. This explains the trend to higher apparent bound water fraction with long T2 saturation preparation pulses compared with UTE acquisition without preparation pulse (8.6% and 5.6% increase, respectively, with half and hard excitation pulses for bovine bone, 10.5% and 7.2% increase, respectively, with half and hard excitation pulses for human bone) or UTE acquisition with a fat saturation preparation pulse (14.4% and 7.7% increase, respectively, with half and hard excitation pulses for bovine bone, 17.1% and 16.7% increase, respectively, with half and hard excitation pulses for human bone).

With adiabatic inversion recovery preparation pulses, there is simultaneous short T2 component excitation and long T2 water and fat suppression. If the repetition time (TR) and inversion time (TI) are appropriate, total suppression of long T2 signal with preservation of short T2 signal should be achieved with the corresponding apparent bound water fraction approaching 100%. In our study, the signals acquired with adiabatic inversion recovery were best fitted with a monoexponential decay model. However, when a biexponential decay model was used post hoc, the monoexponential T2* values were comparable to the short T2* values obtained by the bicomponent analysis model. For instance, on the bovine bone shown in Fig. 3, single component fitting of the half-excitation and hard-excitation inversion recovery sequences yielded T2* values of 0.35 and 0.34 ms, respectively. With a bicomponent fitting model, the short T2* values obtained were 0.32 ms (5.3% shorter) and 0.30 ms (6.6% shorter) for the half-excitation and hard-excitation inversion recovery sequences, respectively. The apparent bound water fraction approaches 100%, confirming the efficient suppression of free water. Free water has approximately 10 times longer T2* compared with bound water and its longitudinal magnetization is partly inverted and nulled by the adiabatic inversion recovery sequence.

In comparison to the other preparation pulses used in this study, we have found that IR-UTE is a dependable technique for effectively separating the bound water from free water compartments in cortical bone, regardless of the pulse type (half excitation versus hard excitation). However, it is important to note that the values of short T2* obtained with IR-UTE are slightly higher than those obtained with UTE bicomponent analyses, suggesting that there is a minor amount of residual free water signal that may contribute to the overall IR-UTE signal. One explanation for this has been recently reported by Horch *et al.*, who found distinct T1 values at 4.7 T for bound water (mean T1s $\sim$357 ms) and free water (mean T1s $\sim$551 ms) in human cortical bone specimens.[34]

There are challenges with regards to the study of the single and bicomponent behavior of T1 relaxation in cortical bone.[17,34] An understanding of their effects on free water suppression will require further investigation. In the future, our efforts will focus on several aspects, including to investigate the relationship between varying inversion time, T2* values, and bound water fractions. If TI is precisely at the nulling point, the bicomponent analysis model will produce

information from only the bound water compartment.[17,34] Consideration should also be given to the degree of field strength inhomogeneity and its effects on the T2* relative bound water fraction.

## 5. CONCLUSION

The UTE sequence without and with preparation pulses (fat saturation, long T2 water saturation, and adiabatic inversion recovery) can detect signal from cortical bone. The UTE bicomponent analysis model provides information on T2*s and the relative bound water fraction of the cortical bone. The type of excitation pulse (half-excitation or hard excitation) significantly affects single-component T2* quantification. The excitation pulse can also potentially affect bicomponent T2* quantification. All three preparation pulses can suppress undesired signal, but the UTE sequence with adiabatic inversion recovery is most efficient in minimizing long T2 signal. The shape of the excitation pulse does not significantly affect the relative fraction of bound water of the IR-UTE sequence. This technique may be useful for effectively separating the bound water in the cortical bone.

## ACKNOWLEDGMENTS

The authors thank grants support from GE Healthcare, 1R01 AR062581-01A1 and 1R21 AR063894-01A1. Shihong Li was supported by the Outstanding Young and Middle-Aged University Teachers and Presidents Training Abroad Project and the Qing Lan Project of Jiangsu Province. Eric Y. Chang was supported by the Career Development Award from the Veterans Affairs Clinical Science Research and Development Service (Grant No. 1IK2CX000749-01).

[a]Author to whom correspondence should be addressed. Electronic mail: jiangdu@ucsd.edu; Telephone: (619) 471-0519; Fax: (619) 471-0503.

[1]M. Srivastava and C. Deal, "Osteoporosis in elderly: Prevention and treatment," Clin. Geriatr. Med. **18**(3), 529–555 (2002).
[2]P. D. Miller and M. McClung, "Prediction of fracture risk. I: Bone density," Am. J. Med. Sci. **312**(6), 257–259 (1996).
[3]J. Smith and K. Shoukri, "Diagnosis of osteoporosis," Clin. Cornerstone **2**(6), 22–33 (2000).
[4]M. C. van der Meulen, K. J. Jepsen, and B. Mikic, "Understanding bone strength: Size isn't everything," Bone **29**(2), 101–104 (2001).
[5]J. D. Currey, "The effects of drying and re-wetting on some mechanical properties of cortical bone," J. Biomech. **21**(5), 439–441 (1988).
[6]S. R. Elliott and R. A. Robinson, "The water content of bone. I. The mass of water, inorganic crystals, organic matrix, and CO2 space components in a unit volume of the dog bone," J. Bone Joint Surg. Am. **39A**(1), 167–88 (1957).
[7]P. A. Timmins and J. C. Wall, "Bone water," Calcif. Tissue Res. **23**(1), 1–5 (1977).
[8]M. A. Morris, J. A. Lopez-Curto, S. P. Hughes, K. N. An, J. B. Bassingthwaighte, and P. J. Kelly, "Fluid spaces in canine bone and marrow," Microvasc. Res. **23**(2), 188–200 (1982).
[9]W. C. Bae, P. C. Chen, C. B. Chung, K. Masuda, D. D'Lima, and J. Du, "Quantitative ultrashort echo time (UTE) MRI of human cortical bone: Correlation with porosity and biomechanical properties," J. Bone Miner. Res. **27**(4), 848–857 (2012).
[10]A. Techawiboonwong, H. K. Song, M. B. Leonard, and F. W. Wehrli, "Cortical bone water: *in vivo* quantification with ultrashort echo-time MR imaging," Radiology **248**, 824–833 (2008).
[11]S. Lenk, S. Fischer, I. Kotter, C. D. Claussen, and H. P. Schlemmer, "Possibilities of whole-body MRI for investigating musculoskeletal diseases," Radiologe **44**(9), 844–853 (2004).
[12]A. Ziemianski and J. Bruszewski, "Indications for magnetic resonance imaging in diseases of the musculoskeletal system," Chir. Narzadow Ruchu Ortop. Pol. **58**(1), 41–45 (1993).
[13]S. Lees, "A mixed packing model for bone collagen," Calcif. Tissue Int. **33**(6), 591–602 (1981).
[14]M. D. Robson, P. D. Gatehouse, M. Bydder, and G. M. Bydder, "Magnetic resonance: An introduction to ultrashort TE (UTE) imaging," J. Comput. Assist. Tomogr. **27**(6), 825–846 (2003).
[15]H. Cao, J. L. Ackerman, M. I. Hrovat, L. Graham, M. J. Glimcher, and Y. Wu, "Quantitative bone matrix density measurement by water- and fat-suppressed proton projection MRI (WASPI) with polymer calibration phantoms," Magn. Reson. Med. **60**, 1433–1443 (2008).
[16]J. S. Nyman, Q. Ni, D. P. Nicolella, and X. Wang, "Measurements of mobile and bound water by nuclear magnetic resonance correlate with mechanical properties of bone," Bone **42**(1), 193–199 (2008).
[17]J. Du and G. M. Bydder, "Qualitative and quantitative ultrashort-TE MRI of cortical bone," NMR Biomed. **26**, 489–506 (2013).
[18]R. A. Horch, D. F. Gochberg, J. S. Nyman, and M. D. Does, "Non-invasive predictors of human cortical bone mechanical properties: T(2)-discriminated H NMR compared with high resolution X-ray," PLoS One **6**(1), e16359 (2011).
[19]R. A. Horch, J. S. Nyman, D. F. Gochberg, R. D. Dortch, and M. D. Does, "Characterization of 1H NMR signal in human cortical bone for magnetic resonance imaging," Magn. Reson. Med. **64**(3), 680–687 (2010).
[20]E. Diaz, C. B. Chung, W. C. Bae, S. Statum, R. Znamirowski, G. M. Bydder, and J. Du, "Ultrashort echo time spectroscopic imaging (UTESI): An efficient method for quantifying bound and free water," NMR Biomed. **25**, 161–168 (2012).
[21]S. Li, E. Y. Chang, W. C. Bae, C. B. Chung, S. Gao, S. Bao, G. M. Bydder, Y. Hua, and J. Du, "Ultrashort echo time bi-component analysis of cortical bone—A field dependence study," Magn. Reson. Med. (2013) [Published online April 29, 2013].
[22]M. Carl, M. Bydder, J. Du, A. Takahashi, and E. Han, "Optimization of RF excitation to maximize signal and T2 contrast of tissues with rapid transverse relaxation," Magn. Reson. Med. **64**, 481–490 (2010).
[23]M. Carl, M. Bydder, J. Du, and E. Han, "Radiofrequency pulses for simultaneous short T2 excitation and long T2 suppression," Magn. Reson. Med. **65**(2), 531–537 (2011).
[24]P. E. Larson, S. M. Conolly, J. M. Pauly, and D. G. Nishimura, "Using adiabatic inversion pulses for long-T2 suppression in ultrashort echo time (UTE) imaging," Magn. Reson. Med. **58**(5), 952–961 (2007).
[25]P. E. Larson, P. T. Gurney, K. Nayak, G. E. Gold, J. M. Pauly, and D. G. Nishimura, "Designing long-T2 suppression pulses for ultrashort echo time imaging," Magn. Reson. Med. **56**(1), 94–103 (2006).
[26]A. Anastasiou and L. D. Hall, "Optimisation of T2 and M0 measurements of bi-exponential systems," Magn. Reson. Imaging **22**(1), 67–80 (2004),
[27]S. J. Graham, P. L. Stanchev, and M. J. Bronskill, "Criteria for analysis of multicomponent tissue T2 relaxation data," Magn. Reson. Med. **35**(3), 370–378 (1996).
[28]K. P. Whittall and A. L. MacKay, "Quantitative interpretation of NMR relaxation data," J. Magn. Reson. **84**(1), 134–152 (1989).
[29]J. Sijbers and A. J. den Dekker, "Maximum likelihood estimation of signal amplitude and noise variance from MR data," Magn. Reson. Med. **51**(3), 586–594 (2004).
[30]R. Biswas, W. Bae, E. Diaz, K. Masuda, C. B. Chung, G. M. Bydder, and J. Du, "Ultrashort echo time (UTE) imaging with bi-component analysis: Bound and free water evaluation of bovine cortical bone subject to sequential drying," Bone **50**(3), 749–755 (2012).
[31]P. Fantazzini, R. J. Brown, and G. C. Borgia, "Bone tissue and porous media: Common features and differences studied by NMR relaxation," Magn. Reson. Imaging **21**(3–4), 227–234 (2003).
[32]J. Du, A. M. Takahashi, M. Bydder, C. B. Chung, and G. M. Bydder, "Ultrashort TE imaging with off-resonance saturation contrast (UTE-OSC)," Magn. Reson. Med. **62**(2), 527–531 (2009).
[33]R. Harrison, M. J. Bronskill, and R. M. Henkelman, "Magnetization transfer and T2 relaxation components in tissue," Magn. Reson. Med. **33**(4), 490–496 (1995).
[34]R. A. Horch, D. F. Gochberg, J. S. Nyman, and M. D. Does, "Clinically compatible MRI strategies for discriminating bound and pore water in cortical bone," Magn. Reson. Med. **68**(6), 1774–1784 (2012).